Relocation of long-period (LP) seismic events reveals en echelon fractures in the upper edifice of Turrialba volcano, Costa Rica

M. Zecevic, L. de Barros, Thomas S. Eyre, I. Lokmer, Christopher J. Bean

AGU PUBLICATIONS

Geophysical Research Letters

RESEARCH LETTER
10.1002/2016GL070427

Key Points:
- Family of LP events relocated using cross-correlation location method
- Source locations jointly interpreted with source mechanisms
- The imaged en echelon structure is a response to deformation in the upper edifice

Supporting Information:
- Supporting Information S1
- Figure S1
- Figure S2
- Figure S3

Correspondence to:
M. Zecevic,
megan.zecevic@ucalgary.ca

Citation:
Zecevic, M., L. De Barros, T. S. Eyre, I. Lokmer, and C. J. Bean (2016), Relocation of long-period (LP) seismic events reveals en echelon fractures in the upper edifice of Turrialba volcano, Costa Rica, *Geophys. Res. Lett.*, *43*, 10,105–10,114, doi:10.1002/2016GL070427.

Received 7 SEP 2015
Accepted 8 SEP 2016
Accepted article online 10 SEP 2016
Published online 6 OCT 2016

Relocation of long-period (LP) seismic events reveals en echelon fractures in the upper edifice of Turrialba volcano, Costa Rica

Megan Zecevic[1,2], Louis De Barros[1,3], Thomas S. Eyre[1,4], Ivan Lokmer[1], and Christopher J. Bean[1,5]

[1]Seismology Laboratory, School of Geological Sciences, University College Dublin, Dublin, Ireland, [2]Now at Department of Geoscience, University of Calgary, Calgary, Alberta, Canada, [3]Now at Université Côte d'Azur, CNRS, OCA, IRD, Géoazur, Sophia-Antipolis, France, [4]Now at Department of Physics, University of Alberta, Edmonton, Alberta, Canada, [5]Now at Geophysics Section, School of Cosmic Physics, Dublin Institute for Advanced Studies, Dublin, Ireland

Abstract Swarms of long-period (LP) events were recorded on Turrialba volcano, Costa Rica, during a seismic field experiment in 2009. Families of LP events were previously identified and located using a joint inversion for source location and mechanism; however, the spatial resolution of the obtained locations was not sufficient for imaging the structures on which they occur. Using a waveform similarity-based location method, we take advantage of the joint location-mechanism inversion by relocating events around the obtained familial location. The location method is successfully tested on a synthetic data set and is then applied to the Turrialba LP data set. The relocated events are jointly interpreted with their source mechanisms and reveal an en echelon structure within the upper edifice of the volcano. This can be interpreted as a response of a shearing band with high fluid pressure inducing tensile fractures at unconsolidated rock layer interfaces within the upper edifice of the volcano.

1. Introduction

Long-period (LP) events are commonly observed on active volcanoes. These signals mainly differ from volcano-tectonic events (i.e., "classical" shear earthquakes) by their dominant low-frequency content (between 0.5 and 5 Hz) with a lack of high frequencies. The number of recorded LP events tends to increase just before or during eruptions, resulting in LP swarms [*McNutt*, 2005]. The study of LP events is therefore crucial to broaden our understanding of the physical processes occurring within the volcano before an eruption in order to improve eruption forecasts. However, the source processes of LP events are still under debate as several source models currently exist. The prominent theory is that LPs are a manifestation of resonance of fluid-filled cavities such as cracks and conduits [*Chouet*, 1986, 1988]. A more recent model suggests that LP events can indicate slow failures in the compliant material of the upper volcanic edifice in order to accommodate deformation [*Bean et al.*, 2014]. One of the most fundamental steps in LP event analysis is determining their source locations. Accurate source locations can provide constraints on the depth, size, and geometry of the source areas and can hence provide insights on the processes involved. Moreover, LP events often occur as families of similar events, which are deemed to have similar source mechanisms and source locations which are $< \lambda/4$ apart, where λ is the seismic wavelength [*Geller and Mueller*, 1980]. By locating these families of LP events we can potentially image their source structures within the volcano [e.g., *De Barros et al.*, 2009].

LP events are characterized by their emergent onset and lack of clear *S* wave arrivals [*Chouet*, 2003]; therefore, traditional location techniques using first-arrival onsets are very challenging and sometimes impossible to apply to LP events. For example, locating similar events using only first-arrival times often results in the obtained source locations being widely scattered within the volcanic edifice [*Battaglia et al.*, 2003]. This happens because picking the first-arrival times of LP events is a very imprecise procedure due to the emergent onset, the low-frequency content, and a low signal-to-noise ratio. Attempts have however been made by *Jousset et al.* [2013] and *Syahbana et al.* [2014] to obtain more accurate and unbiased picking of LP events using Akaike information criteria. Nevertheless, alternative location methods have thus been developed and applied to locate LP events. They are based on array analysis [e.g., *Métaxian et al.*, 2002], waveform similarities [e.g., *Battaglia et al.*, 2003; *De Barros et al.*, 2009; *Matoza et al.*, 2014; *Zecevic et al.*, 2013], or amplitude decay [e.g., *Battaglia and Aki*, 2003; *Battaglia et al.*, 2003]. The location and mechanisms of families of LP events are also commonly investigated using joint moment tensor inversion (MTI) methods [e.g., *Eyre et al.*,

2013; *Kumagai et al*., 2002]. However, the location resolution of the latter method is generally poor; therefore, the structures on which the events are generated cannot be inferred. Joint moment tensor inversion therefore provides the source mechanisms and an absolute, but not precise, location.

In this study we aim to take advantage of previously obtained joint location-mechanism inversion results by relocating events relative to the obtained absolute familial location. By exploiting the similarity between events, the relative source locations of closely spaced events can be better determined as they only depend on the seismic velocity within the source region rather than along the whole raypath. This is a real advantage for volcanoes, where velocity models are usually poorly constrained. A location method, based on waveform similarity techniques [*Got et al*., 1994; *Shearer*, 1997; *Waldhauser and Ellsworth*, 2000], is therefore presented. This method is computationally light and easily implemented. The location method is initially tested on a synthetic family of LP events and is then applied to a real data set of LP events recorded in 2009 on Turrialba volcano, Costa Rica, that was jointly inverted for source location and mechanism by *Eyre et al*. [2013]. The events show an en echelon structure, which can be interpreted as a response of a shearing band together with high fluid pressure within the upper edifice of the volcano.

2. Data

2.1. Turrialba Volcano

Turrialba volcano is a basaltic-andesitic stratovolcano located at the eastern edge of the Cordillera Volcánica Central, Costa Rica. The summit of Turrialba volcano is 3340 m above sea level and is characterized by three craters, named Northeast, Central, and Southwest according to their relative geographical positions within the summit region. From 1996 onward, Turrialba volcano began to show enhanced fumarolic activity combined with increasing levels of seismicity.

Swarms of LP events have been observed on Turrialba by *Martini et al*. [2010], *Soto and Mora* [2013], and *Eyre et al*. [2013, 2015]. A seismic field experiment was carried out between 19 March and 8 September 2009 at Turrialba volcano, whereby 13 stand-alone broadband seismometers were deployed on the volcano (Figure 1a). All sensors were Guralp 6TD 30 s instruments except CIMA, CIM2, and CEN1, which were Guralp 3ESPDC 60 s instruments, and were recording at a sampling rate of 100 Hz. At the time of the experiment, strong fumarolic activity was present in the Southwest crater; however, there were no indications of magmatic activity [*Soto and Mora*, 2013]. Over 6000 LP events, with dominant frequencies between 0.3 and 1.3 Hz (on raw velocity seismograms; Figure S1 in the supporting information), were identified by *Eyre et al*. [2013]; 435 of these events were characterized into a single family of similar events. The family of events, which consisted of five subfamilies, was obtained using cross correlation and cluster analysis for events with a correlation coefficient >0.8. The families of events were inverted for both source location and mechanism using 3-D full-waveform moment tensor inversion, assuming a homogenous *P* wave velocity of 3000 ms^{-1} and including a topographical digital elevation model (DEM) of Turrialba volcano. The hypocenters of the subfamilies of events were similarly positioned beneath the active Southwest and Central craters at depths less than 800 m beneath the summit. The sources of the LP events were determined to be subhorizontal crack mechanisms dipping toward the southwest at angles of approximately 10 to 20°.

A further study was carried out by *Eyre et al*. [2015] on the source mechanisms of LP events on Turrialba volcano recorded during a later field campaign in 2011 using a purposefully designed seismic network to obtain more accurate moment tensor inversion results. Similar locations and mechanisms were found, but no families of more than five events could be identified in this data set.

2.2. LP Data Set

In this study the 2009 Turrialba LP data set analyzed by *Eyre et al*. [2013] is used. Prior to analysis, waveforms are band-pass filtered between 0.3 and 1.3 Hz, the dominant frequency range of the events (Figure S1). After closer examination of the LP event families, it is decided that the 0.8 correlation coefficient threshold used in their study is not sufficient for this location technique to work well, as all of the events within the family are not visually similar at some of the stations located on the flank of the volcano. Closed-cluster analysis (a cross-correlation technique used to classify similar events above an arbitrary threshold into a family, where all events within a family correlate with each other [*Saccorotti et al*., 2007]) is therefore performed again, using summit station CIMA, to obtain event families with a correlation coefficient greater than 0.9. This ensures that

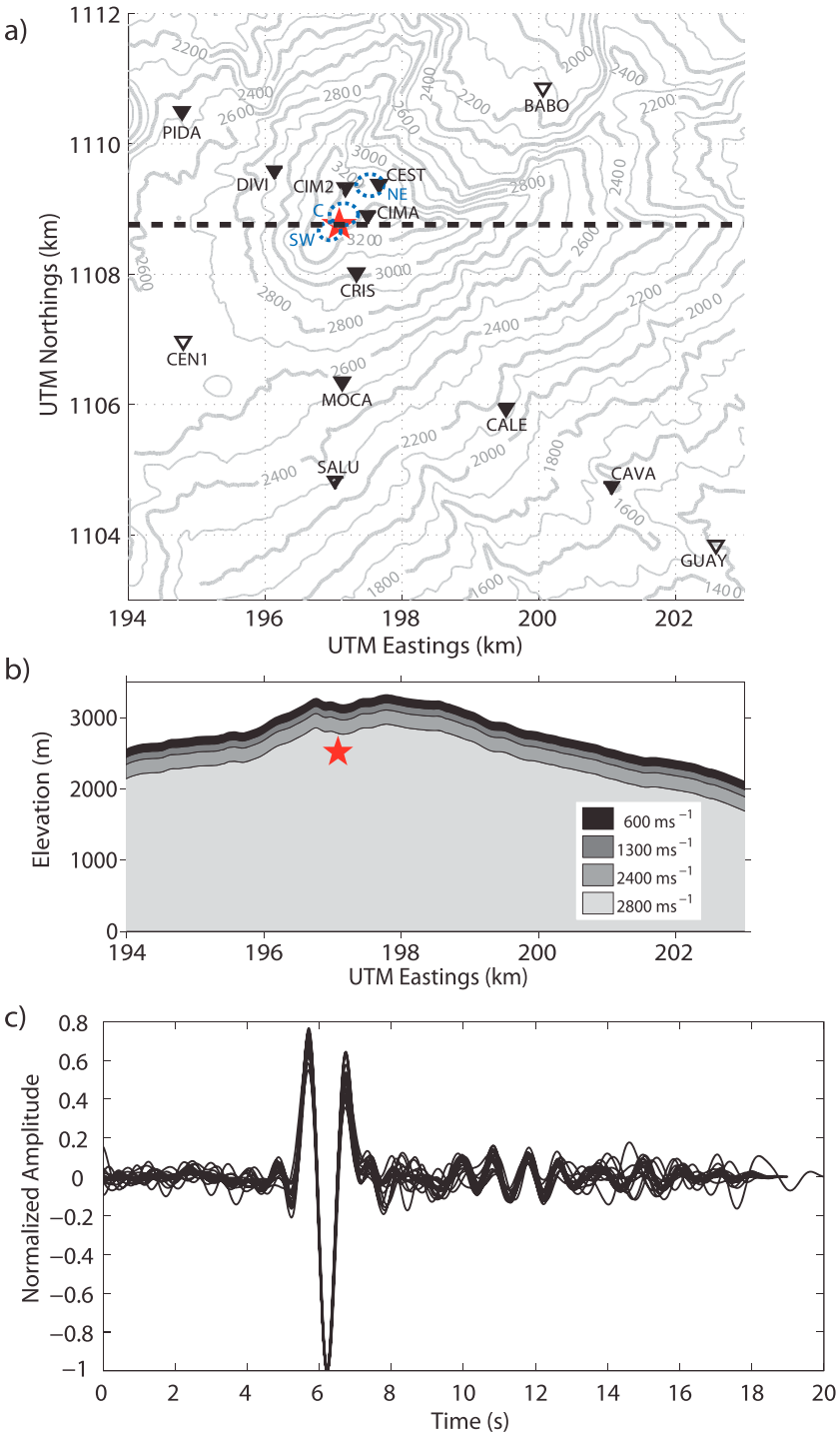

Figure 1. Temporary seismic network on Turrialba volcano used to record LP events in 2009. (a) Map view of Turrialba volcano; the contour lines are in meters above sea level. The triangles illustrate the locations of the seismic stations; the closed triangles are the stations used in the relocation method. The red star represents the source location of the synthetic LP events. The blue dashed circles indicate the approximate locations of the Southwest (SW), Central (C), and Northeast (NE) craters. (b) Cross-sectional view from the south, along the thick dashed line in Figure 1a, illustrating the layered-velocity model used in the synthetic data set and the depth of the synthetic LP source locations with respect to the topography. (c) Aligned waveforms of a family of 17 LP events, with correlation coefficient >0.9, recorded on the vertical component of station CIMA. Waveforms are band-pass filtered between 0.3 and 1.3 Hz.

a "close" family of events is obtained (Figure 1c), with a correlation >0.7 for nearly all events at each station across the network. Five different families of events, similar to the five subfamilies found by *Eyre et al*. [2013] [see *Eyre et al*., 2013, Figure 4a], are once again obtained using this analysis, with 8 events in family 1, 62 events in family 2, 33 events in family 3, 11 events in family 4, and 18 events in family 5. Unfortunately, due to unplanned station downtime the network of operational stations varied frequently throughout the project and there were no more than 10 stations operating at any one time [*Eyre et al*., 2013]. As station distribution can strongly influence the accuracy of obtained source locations. The events are sorted according to the largest network of operational stations by which they were recorded. This ensures that the same station distribution with the greatest spatial coverage is used for relocating all events. Consequently, each station distribution only samples a small subset of the event families. The station distribution that excludes BABO, CEN1, and GUAY recorded the largest number of events, with only 17 events remaining in family 2 and only 3 to 4 events remaining in the other families. The location method is therefore only applied to the family of 17 events using the station configuration shown in Figure 1a without stations BABO, CEN1, and GUAY.

3. Methodology

The principles behind the waveform similarity location methods described by *Shearer* [1997] and *Waldhauser and Ellsworth* [2000] and the cross-correlation location method described by *De Barros et al*. [2009] are used and modified herein in order to locate a family of LP events. First, we determine interevent delay times for all pairs of similar events at each station by finding the maximum of the waveform cross-correlation function for a 3.5 s window surrounding the onset of the event, based on preliminary first-arrival picking. A spline interpolation is applied to the cross-correlation function to obtain a delay time with higher precision than the sampling rate of the signals. The high-correlation coefficient used during cluster analysis prevents any cycle jumps, which is checked during visual screening.

The difference in interevent delay times Δt_{ij} between a pair of stations, *A* and *B*, is exactly the difference in interstation delay times Δt^{AB} between two events *i* and *j*:

$$\Delta t_{ij}^{A} - \Delta t_{ij}^{B} = \Delta t_{i}^{AB} - \Delta t_{j}^{AB}. \tag{1}$$

To locate an individual event, we need to isolate the interstation delay time Δt_i^{AB} for that event. However, solving equation (1) to extract Δt_i^{AB} is an underdetermined problem; therefore, a priori interstation delay times $\Delta \hat{t}_i^{AB}$ are used to stabilize the equation. The a priori delay times are calculated using the MTI source location in the same velocity model as used in the MTI, for the sake of consistency. However, to stabilize the inversion, it is sufficient to add just one a priori delay time for which the most accurate travel times can be determined. This is another advantage associated with this particular method.

Using an example of a family containing three LP events, recorded on a pair of stations labeled *A* and *B*, equation (1) together with the constraints brought by the MTI absolute location can be written explicitly as

$$\begin{bmatrix} \Delta \hat{t}_1^{AB} \\ \Delta t_{12}^{A} - \Delta t_{12}^{B} \\ \Delta t_{13}^{A} - \Delta t_{13}^{B} \\ \Delta t_{23}^{A} - \Delta t_{23}^{B} \end{bmatrix} = \begin{bmatrix} 1 & 0 & 0 \\ 1 & -1 & 0 \\ 1 & 0 & -1 \\ 0 & 1 & -1 \end{bmatrix} \cdot \begin{bmatrix} \Delta T_1^{AB} \\ \Delta T_2^{AB} \\ \Delta T_3^{AB} \end{bmatrix} \tag{2}$$

where ΔT_i^{AB} is the adjusted interstation delay time for event *i* that we need to determine and which will be used later in the location process. Equation (2) can be expressed in matrix form as

$$\boldsymbol{d} = \boldsymbol{G}\boldsymbol{m} \tag{3}$$

where the data vector $\boldsymbol{d}$ contains the a priori interstation delay times and the differential interevent delay times, $\boldsymbol{G}$ is an auxiliary matrix, and $\boldsymbol{m}$ is the model vector which contains the adjusted interstation delay times. Equation (3) can be solved by using a weighted least squares solution:

$$\boldsymbol{m} = \left(\boldsymbol{G}^{T}\boldsymbol{W}\boldsymbol{G}\right)^{-1}\boldsymbol{G}^{T}\boldsymbol{W}\boldsymbol{d} \tag{4}$$

where $\boldsymbol{W}$ is a vector of weights. As the a priori interstation delay times are up to 2 orders of magnitude greater than the differential interevent delay times, their weights are reduced to 0.05. The differential interevent

delay times, measured by cross correlation, are weighted according to the correlation coefficient C between events i and j, as $W_{ij}^{AB} = \min\left(C_{ij}^{A}, C_{ij}^{B}\right)$.

The adjusted interstation delay times, obtained by solving equation (3), are then used to individually relocate each event. For the location procedure a volume bounded by the volcano's topography, obtained from a DEM, is discretized into a grid where each grid point is a potential source location. The synthetic travel time between each grid point and each receiver is calculated, and the subsequent theoretical interstation delay time is determined. This calculation is only performed once as it can be used for all events. As the velocity model in the shallow part of volcanoes are often poorly known, and to keep consistency with the MTI, we here assume a homogeneous velocity model. Alternatively, theoretical interstation delay times can also be computed using an external ray tracer for a heterogeneous velocity structure (if known) and used at this stage.

The most likely source location is determined by the grid point which minimizes the squared difference between the adjusted and theoretical interstation delay times. The following definition is used to determine the squared error:

$$\mathrm{SQE} = \frac{\sum_{n=1}^{N} w_n \left(\Delta T_n^{\mathrm{obs}} - \Delta T_n^{\mathrm{theo}}\right)^2}{\sum_{n=1}^{N} \left(\Delta T_n^{\mathrm{obs}} \times w_n\right)^2} \tag{5}$$

where ΔT^{obs} is the observed (i.e., adjusted; derived from equation (3)) interstation delay time, ΔT^{theo} is the theoretical (i.e., synthetic) interstation delay time from the grid point to the pair of stations, w is derived from the weight associated with the quality of the interevent delay times used in equation (4) ($w = 1/[1 - W]$), and N is the number of pairs of stations.

4. Synthetic Tests

4.1. Synthetic Data Set

As families of events share close source locations, nine closely spaced point sources are used to compute a family of events. A 3×3 grid of sources is used to emulate a 45° eastward dipping planar structure (Figure S2), with 20 m spacing between each row of sources in both the horizontal and vertical directions. The uppermost sources on the inclined plane are positioned at a depth of 700 m beneath the active Southwest crater (Figure 1), which is within the reasonable LP source location range for Turrialba volcano as found by *Eyre et al*. [2013]. Contrary to the MTI results of *Eyre et al*. [2013], the source mechanisms of the nine synthetic events are modeled as vertical tensile cracks rather than subhorizontal cracks. Vertical tensile cracks have anisotropic radiation patterns for all wave types (near-field *P* and *S* waves, intermediate-field *P* and *S* waves, far-field *P* and *S* waves, and surface waves) [*Lokmer and Bean*, 2010], thus resulting in a stronger variation between the synthetic waveforms laterally across the network. A Ricker wavelet with a dominant frequency of 1 Hz is assumed as the source time function.

The topographical effects are intrinsically considered in the synthetic data by including the same DEM of Turrialba volcano previously used by *Eyre et al*. [2013]. To test the influence of unknown velocity model heterogeneities, a layered velocity model consisting of four layers tracking the topography is used in the forward model. The two shallowest layers have a thickness of 100 m, the third layer is 200 m thick, and the bottommost layer acts as a homogeneous half-space, with *P* wave velocities increasing with depth from 600 m/s to 2800 m/s (see Figure 1b). Note that the synthetic LP source locations are situated in the half-space layer. This velocity model is chosen in order to reflect the shallow, low-velocity layers typically observed on volcanoes [*Bean et al*., 2008]. We will later use homogeneous velocity models in the location process, as is usually done when the velocity model is unknown.

The station distribution is based on the same seismic network geometry deployed on Turrialba volcano, Costa Rica, in 2009 (Figure 1a). Synthetic waveforms are computed using 3-D full-waveform simulations by means of an elastic lattice method [*O'Brien and Bean*, 2004] from each point source to each seismic station.

4.2. Synthetic Location Tests

The familial location, i.e., the proxy for the location obtained from MTI, is set as the southwesternmost point source in the planar structure. To locate the synthetic data we first use a velocity of 2800 ms^{-1}, which is the

velocity of the half-space in which the synthetic sources are located. Using these parameters the family of synthetic LP events is successfully relocated and the planar structure is perfectly recovered (Figure S2). We then test the sensitivity to an incorrect homogeneous velocity, which can affect the position of the relocated events, and hence the shape of the imaged structure. A fast velocity results in larger interevent distances and thus leads to a longer structure being imaged. As velocity errors lead to greater errors in the vertical direction, the structure is also more steeply dipping (~56° for a velocity of 3800 ms^{-1}). Inversely, a slower velocity results in a shorter, more shallowly dipping (~27° for a velocity of 2000 ms^{-1}) planar structure being observed. We estimate a location error of less than 20 m for an error of 500 ms^{-1} in the velocity, while a velocity error of 100 ms^{-1} leads to a relative error of less than 10 m. The relative locations are therefore quite robust with changes in velocity. Hence, a homogenous velocity is suitable for relocating LP events and imaging the structures on which they occur.

The effect of using an incorrect absolute location is also tested, assuming that the correct velocity is used. If the absolute location is misplaced by several hundred meters laterally of the true synthetic source location, then the planar structure can still be correctly obtained about the misplaced absolute location. However, if the absolute location is significantly different from the true absolute location ($>$1 km) so that its relative position to several stations in the seismic network has drastically changed, then the obtained planar structure can be completely distorted. For example, when the absolute position is misplaced 975 m laterally toward the summit stations and 360 m vertically upward from the true synthetic source location, the obtained relative locations appear correct on the horizontal plane; however, the recovered source locations are misplaced on the vertical plane so that the obtained structure is dipping 45° westward rather than 45° eastward (Figure S3). The method therefore seems robust for relatively locating events, assuming that the absolute location is not drastically wrong.

Uncertainties in location due to potential noise in the event waveforms (as a result of poor signal-to-noise ratio or potential filtering effects) are determined using a Monte Carlo simulation assuming a Gaussian error of 10 ms on the differential interevent delay times for the synthetic data. Relocations are performed 50 times, and correct locations are obtained for all events in 47 out of the 50 iterations; therefore, results are reliable at the 94% confidence level. The three iterations that do not result in correct locations for all events are correct for eight out of nine of the synthetic events. The mislocated event in each of these iterations is displaced by one grid step (20 m) vertically from the true location (Figure S2). The locations are therefore still reliable when errors are present in the differential interevent delay times.

5. Turrialba LP Locations

5.1. Results: Source Locations

The average location obtained by *Eyre et al*. [2013] for the subfamily considered in this study is assumed to be the familial source location. The family of 17 LP events is hence relocated about the assumed familial location beneath the Southwest and Central craters, using the same homogeneous *P* wave velocity of 3000 ms^{-1} employed in the MTI [*Eyre et al*., 2013] and a grid resolution of 20 m. The obtained relative source locations of the LP events are shown in Figure 2 as red dots in map view (Figure 2a) and in a southwest-northeast cross section (Figure 2b). A Monte Carlo simulation, assuming a Gaussian error of 10 ms (~30%) on the differential interevent delay times, is performed to test for uncertainties in the source locations. Over 50 iterations, 13% of the events are offset in the eastward direction by one grid point (±20 m), 4% of the events are displaced by one grid point (±20 m) northward, and 11% of the events are displaced by up to two grid points (±40 m) vertically. The remaining events are located in the same position. As the location errors are relatively small, the overall obtained structure does not change.

The LP event sources define a southwest-northeast trending elongated structure dipping toward the northeast. However, following the synthetic tests, the geometry of the structure may vary in dip angle and vertical extent depending on the velocity used in the location process. Nonetheless, the southwest-northeast trend of the structure and the dip direction are robust as they are insensitive to the velocity used in the location process.

One event does not cluster well with the other LP event locations, both in the horizontal and vertical planes. This event has a very poor signal-to-noise ratio on the flank stations, which can therefore produce large errors

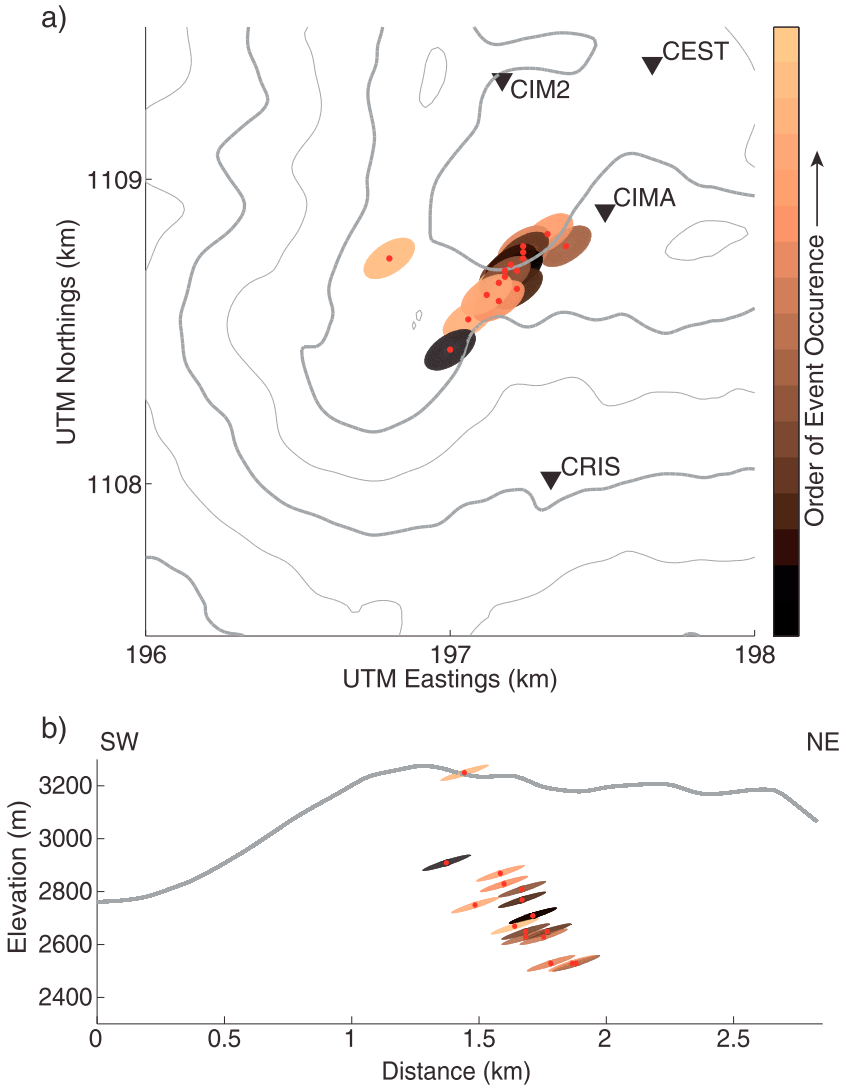

Figure 2. (a) Map view and (b) cross-sectional view of the relocated LP events on Turrialba volcano, Costa Rica. The red dots indicate the obtained source locations. The ellipses illustrate the orientation and approximate extent of the obtained subhorizontal crack mechanism obtained by *Eyre et al.* [2013] and are color coded in order of event occurrence. Cross-sectional view is taken along the southwest-northeast trend defined by the LP event locations.

when computing the delay times. Except for this event, the location structure is ~530 m long. This distance might seem quite large for a family of events; however, as the dominant wavelength is approximately 3000 m, this distance is within the theoretical limits of waveform coherency (i.e., less than a quarter wavelength) [*Geller and Mueller*, 1980].

The elongated structure defined by the LP event locations (herein referred to as the relocation structure) extends from 500 m beneath the southern edge of the Southwest crater (which was the site of a minor phreatic eruption in January 2010 [*Eyre et al.*, 2013]) toward the northeast to a depth of 850 m beneath the southeast rim of the Central crater, with an approximate dip angle of 45°. The occurrence of the LP events in time and space do not appear to show any clear migration pattern (Figure 2).

5.2. Discussion: Relationship Between Source Locations and Mechanisms

Eyre et al. [2013] inverted these LP events for their source mechanisms and obtained subhorizontal crack mechanisms, which are shallowly dipping to the southwest with a dip angle of 10–20°. The obtained crack geometry is superimposed on to the LP event locations as ellipses, assuming a crack length of 100 m, in

Figure 2. Interestingly, the cracks dip toward the southwest, which is opposite to the dip direction of the relocation structure. Such a pattern was also observed at Mount Etna [*De Barros et al*., 2009, 2011] and could potentially be a common feature for LP events on volcanoes. The combined structures suggest that these LP events are similar events originating from distinct sources within a larger structure rather than from a single repeating source. The LP events are therefore generated by multiple sources and are not "nondestructive" repeating events.

The subsequent structure, following the LP source model of *Chouet* [1986], could possibly be a pipe through which rising fluids (e.g., upwelling gas) trigger resonance in the adjacent, orthogonal cracks. Similar models have been proposed by, e.g., *Jousset et al*. [2013] on Merapi volcano. However, *Thun et al*. [2015] showed that the LP events used here contain a significant static displacement component. This observation is not consistent with a pure resonance mechanism. A more likely hypothesis is that these events are generated by tensile (or hybrid mode I–III) failures, in order to accommodate deformation [*Bean et al*., 2014]. This model is coherent with the LP pulse-like waveforms (Figure 1c), the event-size scaling laws, and the transtensional LP source mechanisms obtained by *Eyre et al*. [2015]. In this case, the events define an array of "en echelon" fractures, which is a common pattern in tectonics. Geologically, the cracks on which the LP events are generated could exist due to the presence of layers of old lava flows and tephra that emanated from the Northeast and Central craters (which are aligned N40°E from the Southwest crater) when they were active in the past. The cracks could therefore open along planes of weakness related to the layer interfaces. The opening of subhorizontal cracks requires the presence of high fluid pressure, possibly pertaining to the shallow hydrothermal system, in order to decrease the vertical effective stress. In contrast with the resonating crack model, the fluids are not directly imprinted into the signature of the seismic signals but rather play an important role in modifying the overall stress field within the source zone. A complementary hypothesis might be that these events are related to a shearing band within the volcano. Such extension fractures, with dominant mode I displacement, are commonly observed around tectonic faults [e.g., *Olson and Pollard*, 1991; *Blenkinsop*, 2008]. Consistent with this hypothesis, we find here an angle of about 65° between the tensile crack orientations and the relocation structure along which the LP events trend. Moreover, the trend of the relocation structure found in our study also follows the southwest-northeast trending graben structure (which also has a strike-slip component of motion), in which Turrialba volcano lies [*Soto*, 1988]. The relocation structure might therefore be the shallow signature of movement on these inherited graben structures. Hence, it is possible that the en echelon structure on which the LP events are located might be the result of shearing across material with alternating mechanical properties. However, the link between the tectonic regime and the shallow deformation of the volcano is difficult to discern as the stress regime can be completely modified by the presence of fluids, topographical effects, gravitational instability, and structural heterogeneities near the summit.

6. Discussion and Conclusion

Families of LP events are often located using a joint location-moment tensor inversion [e.g., *Eyre et al*., 2013; *Kumagai et al*., 2002]. The spatial resolution of this inversion is often coarse and is therefore not sufficient for imaging structures within volcanoes. Relocation of LP events, based on a cross-correlation technique, was successfully used to image structures within Mount Etna volcano, Sicily, by *De Barros et al*. [2009]. Here we take advantage of these two methods to relocate LP events around the location obtained by the joint location-moment tensor inversion. The method is computationally light and easily implemented. Through relocations and mechanisms, we are then able to infer in greater detail the structures on which the events occur.

The method is applied to a family of LP events recorded on Turrialba volcano, Costa Rica, during a seismic field experiment in 2009. The LP events are relocated about their familial MTI location determined by *Eyre et al*. [2013]. The locations of the LP events define an elongated structure (orientated with dip and dip direction (i.e., 90° from the strike) of 45°/045°) within the shallow part of the volcano. The geometry of the tensile cracks found through MTI is superimposed onto the relocated structure, revealing en echelon fractures within Turrialba's edifice. In combination with results from previous studies [*Eyre et al*., 2015; *Thun et al*., 2015], we suggest that this structure could be a response to the deformation of the shallow part of the edifice [*Bean et al*., 2014], with a shearing band together with high fluid pressure inducing tensile fractures at

unconsolidated rock layer interfaces. This might be a common feature on volcanoes as similar structures were also observed on Mount Etna [*De Barros et al*., 2011].

The obtained relocation structure, when combined with the source mechanisms obtained through MTI, reveals a detailed geometrical relationship between LP sources, which can be interpreted with respect to a new, recently proposed brittle deformation-based LP source model. This study therefore highlights the need for further LP event studies to implement a more systematic relocation procedure, together with joint interpretation of the source mechanisms, to better infer the source processes of LP events within volcanoes.

Acknowledgments
The research leading to these results has received support from the QUEST Initial Training Network funded within the EU Marie Curie Programme, and Science Foundation Ireland, contract 09/RFP/GEO2242. Field work was partially supported by the projects "Estudio de la evolución geológica y petrológica del volcán Turrialba: implicaciones para la evolución volcánica de Costa Rica y prevención de riesgos volcánicos" (113-A9-509) and "Atenuación sísmica en el volcán Turrialba y su implicación para terrenos volcánicos y en la generación de grandes deslizamientos" (113-A9-508), financed by CONARE (National Council of Rectors from Costa Rica). F. Martini, M. Mora, J. Pacheco, C. Redondo, L. F. Brenes, and G. Soto are acknowledged for their contributions to the field experiment on Turrialba. We do not have full ownership of the seismic data and so do not have the right to distribute it.

References

Battaglia, J., and K. Aki (2003), Location of seismic events and eruptive fissures on the Piton de la Fournaise volcano using seismic amplitudes, *J. Geophys. Res.*, *108*(B8), 2364, doi:10.1029/2002JB002193.

Battaglia, J., J.L. Got, and P. Okubo, (2003), Location of long-period events below Kilauea volcano using seismic amplitudes and accurate relative relocation, *J. Geophys. Res.*, *108*(B12), 2553, doi:10.1029/2003JB002517.

Bean, C. J., L. De Barros, I. Lokmer, J. P. Métaxian, G. S. O'Brien, and S. Murphy (2014), Long-period seismicity in the shallow volcanic edifice formed from slow-rupture earthquakes, *Nat. Geosci.*, *7*, 71–75, doi:10.1038/ngeo2027.

Bean, C., I. Lokmer, and G. O'Brien (2008), Influence of near-surface volcanic structure on long-period seismic signals and on moment tensor inversions: Simulated examples from Mount Etna, *J. Geophys. Res.*, *113*, B08308, doi:10.1029/2007JB005468.

Blenkinsop, T. G. (2008), Relationships between faults, extension fractures and veins, and stress, *J. Struct. Geol.*, *30*, 622–632, doi:10.1016/j.jsg.2008.01.008.

Chouet, B. (1986), Dynamics of a fluid-driven crack in three dimensions by the finite difference method, *J. Geophys. Res.*, *91*(B14), 13,967–13,992, doi:10.1029/JB091iB14p13967.

Chouet, B. (1988), Resonance of a fluid-driven crack: Radiation properties and implications for the source of long-period events and harmonic tremor, *J. Geophys. Res.*, *93*(B5), 4375–4400, doi:10.1029/JB093iB05p04375.

Chouet, B. (2003), Volcano seismology, *Pure Appl. Geophys.*, *160*(3), 739–788, doi:10.1007/PL00012556.

De Barros, L., C. J. Bean, I. Lokmer, G. Saccorotti, L. Zuccarello, G. S. O'Brien, J.-P. Métaxian, and D. Patanè (2009), Source geometry from exceptionally high resolution long period event observations at Mt. Etna during the 2008 eruption, *Geophys. Res. Lett.*, *36*, L24305, doi:10.1029/2009GL041273.

De Barros, L., I. Lokmer, C. J. Bean, G. S. O'Brien, G. Saccorotti, J. P. Métaxian, L. Zuccarello, and D. Patanè (2011), Source mechanism of long-period events recorded by a high-density seismic network during the 2008 eruption on Mount Etna, *J. Geophys. Res.*, *116*, B01304, doi:10.1029/2010JB007629.

Eyre, T. S., C. J. Bean, L. De Barros, G. S. O'Brien, F. Martini, I. Lokmer, M. M. Mora, J. F. Pacheco, and G. J. Soto (2013), Moment tensor inversion for the source location and mechanism of long period (LP) seismic events from 2009 at Turrialba volcano, Costa Rica, *J. Volcanol. Geotherm. Res.*, *258*, 215–223, doi:10.1016/j.jvolgeores.2013.04.016.

Eyre, T. S., C. J. Bean, L. De Barros, F. Martini, I. Lokmer, M. M. Mora, J. F. Pacheco, and G. J. Soto (2015), A brittle failure model for long-period seismic events recorded at Turrialba volcano, Costa Rica, *J. Geophys. Res. Solid Earth*, *120*, 1452–1472, doi:10.1002/2014JB011108.

Geller, R. J., and C. S. Mueller (1980), Four similar earthquakes in central California, *Geophys. Res. Lett.*, *7*, 821–824, doi:10.1029/GL007i010p00821.

Got, J. L., J. Fréchet, and F. W. Klein (1994), Deep fault plane geometry inferred from multiplet relative relocation beneath the south flank of Kilauea, *J. Geophys. Res.*, *99*(B8), 15,375–15,386, doi:10.1029/94JB00577.

Jousset, P., A. Budi-Santoso, A. D. Jolly, M. Boichu, S. Surono, S. Dwiyono, S. H. Sumarti, and P. Thierry (2013), Signs of magma ascent in LP and VLP seismic events and link to degassing: An example from the 2010 explosive eruption at Merapi volcano, Indonesia, *J. Volcanol. Geotherm. Res.*, *261*, 171–192, doi:10.1016/j.jvolgeores.2013.03.014.

Kumagai, H., B. Chouet, and M. Nakano (2002), Waveform inversion of oscillatory signatures in long-period events beneath volcanoes, *J. Geophys. Res.*, *107*(B11), 2301, doi:10.1029/2001JB001704.

Lokmer, I., and C. J. Bean (2010), Properties of the near-field term and its effect on polarization analysis and source locations of long-period (LP) and very-long-period (VLP) seismic events at volcanoes, *J. Volcanol. Geotherm. Res.*, *192*(1–2), 35–47, doi:10.1016/j.jvolgeores.2010.02.008.

Martini, F., F. Tassi, O. Vaselli, R. Del Potro, M. Martinez, R. V. del Laat, and E. Fernandez (2010), Geophysical, geochemical and geodetical signals of reawakening at Turrialba volcano (Costa Rica) after almost 150 years of quiescence, *J. Volcanol. Geotherm. Res.*, *198*(3–4), 416–432, doi:10.1016/j.jvolgeores.2010.09.021.

Matoza, R. S., P. M. Shearer, and P. G. Okubo (2014), High-precision relocation of long-period events beneath the summit region of Kilauea volcano, Hawaii, from 1986 to 2009, *Geophys. Res. Lett.*, *41*, 3413–3421, doi:10.1002/2014GL059819.

McNutt, S. R. (2005), Volcanic seismology, *Annu. Rev. Earth Pl. Sc.*, *33*, 461–491, doi:10.1146/annurev.earth.33.092203.122459.

Métaxian, J.P., P. Lesage, and B. Valette (2002), Locating sources of volcanic tremor and emergent events by seismic triangulation: Application to Arenal volcano, Costa Rica, *J. Geophys. Res.*, *107*(B10), 2243, doi:10.1029/2001JB000559.

O'Brien, G. S., and C. J. Bean (2004), A 3D discrete numerical elastic lattice method for seismic wave propagation in heterogeneous media with topography, *Geophys. Res. Lett.*, *31*, L14608, doi:10.1029/2004GL020069.

Olson, J. E., and D. D. Pollard (1991), The initiation and growth of en échelon veins, *J. Struct. Geol.*, *13*, 595–608, doi:10.1016/0191-8141(91)90046-L.

Saccorotti, G., I. Lokmer, C. J. Bean, G. Di Grazia, and D. Patanè (2007), Analysis of sustained long-period activity at Etna volcano, Italy, *J. Volcanol. Geotherm. Res.*, *160*(3–4), 340–354, doi:10.1016/j.jvolgeores.2006.10.008.

Shearer, P. M. (1997), Improving local earthquake locations using the L1 norm and waveform cross correlation: Application to the Whittier Narrows, California, aftershock sequence, *J. Geophys. Res.*, *102*(B4), 8269–8283, doi:10.1029/96JB03228.

Soto, G. J. (1988), Estructuras volcano-tectónicas del volcan Turrialba, Costa Rica, America Central, in *Actas Quinto Congreso Geológico Chileno*, pp. 163–175, Quinto Congreso Geológico Chileno, Santiago.

Soto, G. J., and M. Mora (2013), Actividad del volcán Turrialba (2007–2011) y perspectivas de amenaza volcánica, in *Costa Rica en el Tercer Milenio: Desafíos y Propuestas Para la Reducción de Vulnerabilidad Ante los Desastres*, pp. 287–310, Preventec, UCR, San José, Calif.

Syahbana, D. K., C. Caudron, P. Jousset, T. Lecocq, T. Camelbeeck, A. Bernard, and Surono (2014), Fluid dynamics inside a "wet" volcano inferred from the complex frequencies of long-period (LP) events: An example from Papandayan volcano, West Java, Indonesia, during the 2011 seismic unrest, *J. Volcanol. Geotherm. Res.*, *280*, 76–89, doi:10.1016/j.jvolgeores.2014.05.005.

Thun, J., I. Lokmer, and C. J. Bean (2015), New observations of displacement steps associated with volcano seismic long-period events, constrained by step table experiments, *Geophys. Res. Lett.*, *42*, 3855–3862, doi:10.1002/2015GL063924.

Waldhauser, F., and W. L. Ellsworth (2000), A double-difference earthquake location algorithm: Method and application to the Northern Hayward Fault, California, *Bull. Seismol. Soc. Am.*, *90*(6), 1353–1368, doi:10.1785/0120000006.

Zecevic, M., L. De Barros, C. J. Bean, G. S. O'Brien, and F. Brenguier (2013), Investigating the source characteristics of long-period (LP) seismic events recorded on Piton de la Fournaise Volcano, La Réunion, *J. Volcanol. Geotherm. Res.*, *258*, 1–11, doi:10.1016/j.jvolgeores.2013.04.009.